Gamma Rays from Lithium Bombardment of Be^9, B^{10}, B^{11}, and C^{12}†

E. NORBECK, S. A. COON, R. R. CARLSON, AND E. BERKOWITZ
Department of Physics and Astronomy, State University of Iowa, Iowa City, Iowa
(Received 23 January 1963)

Relative intensities of gamma rays produced in the bombardment of Be^9, B^{10}, B^{11}, and C^{12} targets by Li^6 and Li^7 beams have been obtained with a three-crystal pair spectrometer and with a single NaI(Tl) crystal. Gamma rays have been observed from excited states in the residual nuclei Li^7, Be^{10}, B^{10}, B^{11}, B^{12}, C^{12}, C^{13}, C^{14}, N^{14}, N^{15}, O^{15}, O^{16}, and O^{17}. Some of these gamma rays have not been observed previously. Relative populations deduced from the data are discussed.

INTRODUCTION

THE bombardment of lithium, beryllium, boron, and carbon by lithium beams of 3-MeV ion energy induces gamma radiation from excited states of residual nuclei formed in nuclear reactions. A study of this radiation gives much information about the reactions which take place, especially relative cross sections for the formation of the individual states of the residual nuclei. Such gamma-ray observations cannot give any information about the formation of the ground state or unbound states; of the latter because the partial width for particle emission is many orders of magnitude larger than that for photon emission.

Although a similar study has been made recently for lithium-lithium reactions,[1] an extensive study of the gamma radiation from lithium bombardment of beryllium, boron, and carbon has not been made previously. The Saclay group has observed gamma rays from Li^6+Be^9 and Li^6+C^{12} at a bombarding energy of 2 MeV with a $1\frac{1}{2}$-in. NaI(Tl) crystal.[2–4] Better results can be obtained from a larger crystal because of its greater efficiency and because a larger fraction of the pulse-height spectrum is in the full-energy-loss peak (photopeak). For gamma rays above 1.02 MeV, a three-crystal pair spectrometer gives a simpler spectrum which can be more easily subjected to an intensity analysis. The three-crystal pair spectrometer eliminates two peaks of the characteristic three-peak response of the NaI(Tl) crystal and reduces the background which is due to a continuous distribution from each gamma ray in the spectrum.

EXPERIMENTAL APPARATUS AND PROCEDURE

Thick targets of elemental Be^9, B^{10}, B^{11}, and C^{12} were bombarded with Li^6 and Li^7 beams from the State University of Iowa 4-MeV Van de Graaff accelerator. The actual bombardment energy ranged from 2.7 to 3.8 MeV. Over this range no change in the shape of the thick-target gamma-ray spectra with beam energy was observed, but for completeness the actual beam energy used is given on each figure.

Spectra of the resulting gamma rays were obtained with a three-crystal pair spectrometer in the energy range of 1 to 10 MeV. The low-energy gamma rays were studied with a single 5-in.-diam×6-in.-long NaI(Tl) crystal. Some gamma rays with energies above 10 MeV were observed. These will be the subject of a forthcoming paper. Energy calibration for the gamma rays was obtained from the self-consistency of the gamma-ray assignments and by the use of low-energy gamma-ray sources.

The three-crystal pair spectrometer, hereafter referred to as the 3CPS, has been described in detail by Carlson and Valerio.[5] It consists of two 5-in.-diam ×3-in.-thick identical NaI(Tl) crystals placed face to face with photomultiplier tubes on the opposite faces. Grooves have been cut across the adjoining faces forming a $2\frac{1}{2}$-in. cylindrical hole in which fits a 2-in.-diam×2-in.-long NaI(Tl) crystal. Gamma rays of sufficient energy can make electron-positron pairs in the 2-in. center crystal. The signal from the center crystal is gated into a 256-channel pulse-height analyzer by a time coincident (50 nsec) capture in the two side crystals of annihilation photons which have escaped from the center crystal. As a pulse is recorded only when both photons escape, the 3CPS suppresses the photopeak and the first escape peak of the gamma ray and reduces the background considerably.

The 3CPS was placed at 0 deg to the direction of the beam with the center crystal viewing the target through the $\frac{1}{16}$-in.-thick brass wall of the target chamber. For the low-energy gamma rays and for the Li^7+B^{10} reaction using the 3CPS the detector viewed the target through a Lucite window at 90 deg to the beam. Except for rather small Doppler shift effects, the spectra looked the same at the two angles. In all cases the distance between the target and the front of the detector was about 3-in.

The relative intensities of gamma rays in the 3CPS spectra were found by numerical integration after subtraction of low-energy tails, using standard shapes,[6]

† Supported in part by the U. S. Atomic Energy Commission.
[1] E. Berkowitz, S. Bashkin, R. R. Carlson, S. A. Coon, and E. Norbeck, Phys. Rev. **128**, 247 (1962).
[2] C. Lemeille, L. Marquez, N. Saunier, and M. Coste, J. Phys. Radium **22**, 349 (1961).
[3] L. Marquez, J. Phys. Radium **21**, 355 (1960).
[4] L. Marquez and Pham-Dinh-Lien, J. Phys. Radium **22**, 589 (1961).
[5] R. R. Carlson and J. I. Valerio, in *Scintillation Spectroscopy of Gamma Radiation*, edited by J. B. Marion (Gordon and Breech, New York, 1963), Chap. V.
[6] J. I. Valerio, thesis, State University of Iowa, 1961 (unpublished).

TABLE I. Li^6+Be^9.

E_γ[a]	Relative intensity[b]	Component intensity[c]	Source[d]	Branching ratio[e]	Direct population[f]
8.70	0.46		B^{11} 8.57 → 0	62	≤0.74
			B^{11} 8.93 — 0		
7.95	0.04	0.06	B^{11} 7.99 → 0	55	0.11[i]
6.97	0.54		N^{14} 7.03 → 0	(100)	0.40
		0.14	B^{11} 7.30 → 0	93	0.15[i]
6.67	0.18	0.18	B^{11} 6.76 → 0 6.81 → 0	83 79	0.18[i]
			(C^{14} 6.72 → 0)	100	
6.40	0.34		N^{14} 6.44 → 0	100	~0.13
		≤0.21	B^{11} 8.57 → 2.14[6.43]	28	cf. 8.70γ
5.80	<0.22	0.05	B^{11} 7.99 → 2.14[5.85]	45	cf. 7.95γ
			(C^{14} 6.09 → 0)	100	
5.04	0.68		N^{14} 4.91 → 0	100	~0.51
		≤0.17	B^{11} 5.04 → 0	88	0.15[i]
			(N^{14} 5.10 → 0)	67	
4.46	0.99		C^{12} 4.43 → 0	100	~0.76
		≤0.19	B^{11} 4.46 → 0	100	0.14[i]
		<0.04	B^{11} 6.81 → 2.14[4.67]	21	cf. 6.67γ
3.89 3.68	3.60		C^{13} 3.85 → 0 C^{13} 3.68 → 0	76 100	3.55
		≤0.05	B^{11} 8.57 → 5.04[3.53]	10	cf. 8.70γ
		0.003	N^{14} 3.95 → 0	4	cf. 1.67γ
3.09	1.00		C^{13} 3.09 → 0	100	0.97
		0.03	B^{11} 5.04 → 2.14[2.89]	12	cf. 5.04γ
2.66			escape peak		
2.25	0.68		N^{14} 2.31 → 0	100	
		≤0.04	B^{11} 6.76 → 4.46[2.30]	17	
2.13	1.20	0.49	B^{11} 2.14 → 0	100	0.08[i]
		≤0.41	B^{10} 2.15 → 0	30	≤1.36
1.83			escape peak		
1.67	0.13		N^{14} 3.95 → 2.31[1.64]	96	0.13
1.48	0.54	≤0.54	B^{10} 2.15 → 0.72[1.43]	40	cf. 2.13γ
			K^{40}		
1.06	1.84		B^{10} 1.74 → 0.72[1.02]	100	1.43
0.83			C^{14} 6.89 → 6.09[0.80]	100	
			g		
0.72	18.6		B^{10} 0.72 → 0	100	16.4
0.48	21.8		Li^7 0.48 → 0	100	21.8
			annihilation radiation		
0.425[h]		≤0.41	B^{10} 2.15 → 1.74[0.41]	30	
			g		
0.210[h]			g		
0.175[h]			C^{14} 3.85 → 3.68[0.17]	24	

[a] Energy of the observed peak in MeV.
[b] Relative area under peak and above background, corrected for detector efficiency.
[c] Fraction of the peak attributed to the single source.
[d] Sources of the observed gamma ray which analysis indicates may contribute significantly to the observed intensity. Parentheses indicate a less certain assignment. The number in brackets is the spacing of the two levels in MeV.
[e] Branching ratio in percent from reference 8.
[f] Direct population of the energy level. This number does not include population by cascade from higher levels. These numbers are on the same scale as the relative intensity. Designated by p.
[g] Gamma rays resulting from the interaction of neutrons with NaI(Tl).
[h] Gamma rays which do not appear on the figures.
[i] Relative populations from reference 10.

and of a smooth, low-energy continuum which was attributed mostly to edge effects. The subtracted peaks are shown in dashed lines on the figures. The final intensities were corrected for the efficiency of the 3CPS. The low-energy single-crystal spectra were subjected to an intensity analysis after a subtraction of the beta and gamma continuum. These figures were corrected for the efficiency and photofraction of a 5-in.×6-in. crystal.[7] For the peaks in the spectrum of the 3CPS above 4 MeV the error in intensities is less than 20%. The error in the intensities of all lower energy gamma rays does not exceed 50%.

[7] W. F. Miller, J. Reynolds, and W. J. Snow, Argonne National Laboratory Report ANL-5902, 1958 (unpublished).

For most reactions the direct population of states in the residual nuclei could be calculated from the intensity of the gamma rays and known gamma-ray branching ratios.[8] For the reactions $C^{12}(Li^6,He^4)N^{14}$ and $C^{12}(Li^7,He^4)N^{15}$, the particle cross sections have been measured for the first three states in N^{14} and N^{15}.[9] For the reaction $Be^9(Li^6,He^4)B^{11}$ the particle cross sections for the first seven excited states in B^{11} have been measured.[10] Because the gamma-ray yields are essentially isotropic, the gamma-ray spectra taken at one

[8] F. Ajzenberg-Selove and T. Lauritsen, Nucl. Phys. **11**, 1 (1959).
[9] R. K. Hobbie and F. W. Forbes, Phys. Rev. **126**, 2137 (1962).
[10] R. K. Hobbie, C. W. Lewis, and J. M. Blair, Phys. Rev. **124**, 1506 (1961).

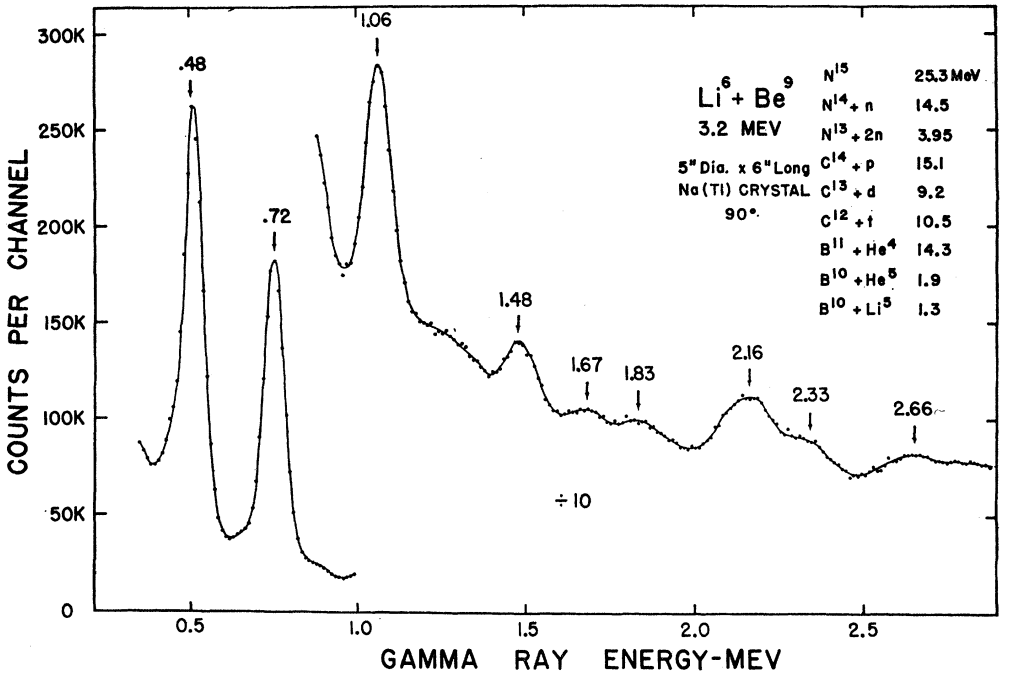

FIG. 1. Gamma rays with energies between 0.5 and 3 MeV from Li^6 bombardment of Be^9. Reactions which are energetically allowed are listed with their Q values.

angle can be directly compared with the integrated particle cross sections. The Li^6+Be^9 reaction discussed here was at a lower bombarding energy than the particle data but there is evidence that the relative cross sections change little with a change in bombarding energy. These direct relative populations appear under the heading "Direct Population" in the tables.

DISCUSSION

Li^6+Be^9

The data are shown in Figs. 1 and 2, and the intensity analysis is given in Table I.

The largest peak in the spectrum is the 0.48-MeV peak. McGrath has shown that annihilation radiation

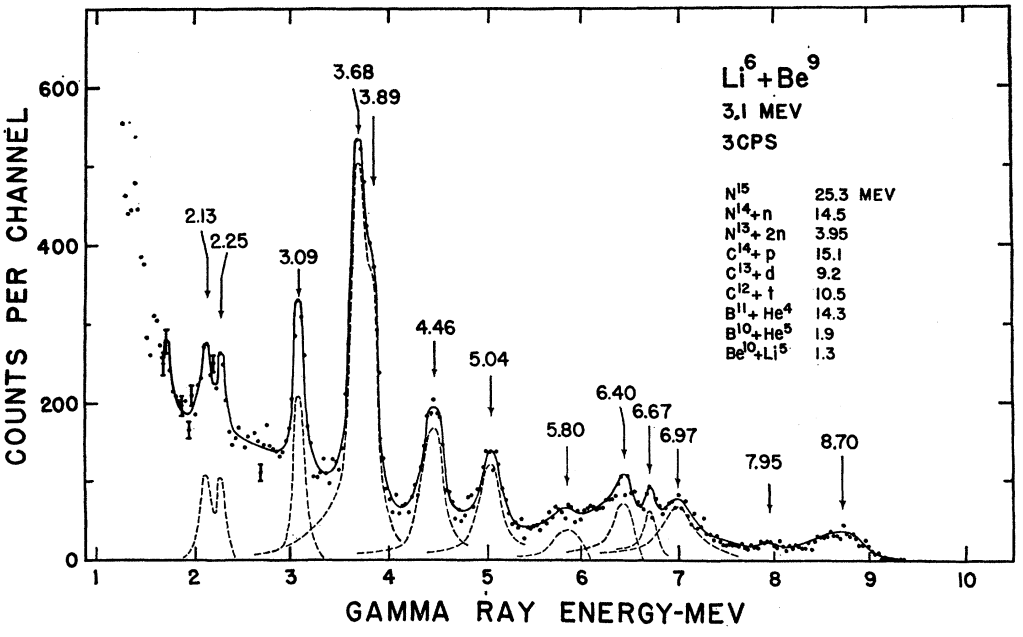

FIG. 2. Gamma rays with energies between 1 and 10 MeV from Li^6 bombardment of Be^9. The possible sources of gamma rays detectable in the 3CPS are listed with the Q values of the reaction. The dashed lines show the subtracted peak shapes, uncorrected for efficiency.

TABLE II. Li^7+Be^9.

E_γ[a]	Relative intensity[b]	Component intensity[c]	Source[d]	Branching ratio[e]	Direct population[f]
6.80	0.78		B^{11} 6.81 → 0	79	
			6.76 → 0	83	
			C^{14} 6.72 → 0	100	
			(B^{11} 7.30 → 0)	93	
			(C^{14} 7.34 → 0)		
6.20	0.36		N^{14} 6.44 → 0	100	
			C^{14} 6.09 → 0	100	
		≤0.04	N^{14} 6.23 → 0	24	≤0.18
	unobservable	0.05	N^{14} 5.69 → 0	37	
5.10	1.19		N^{14} 5.10 → 0	67	
			B^{11} 5.04 → 0	88	
4.46	1.00		B^{11} 4.46 → 0	100	
			C^{12} 4.43 → 0	100	
			B^{11} 6.81 → 2.14[4.67]	21	
3.88	0.14		N^{14} 6.23 → 2.31[3.92]	76	
			C^{13} 3.85 → 0	76	
			3.68 → 0	100	
			N^{14} 3.95 → 0	04	
3.38	0.09		N^{14} 5.69 → 2.31[3.38]	33	0.14
2.84	0.32		B^{11} 5.04 → 2.14[2.90]	12	
			N^{14} 5.10 → 2.31[2.79]	33	
			(B^{11} 7.30 → 4.46[2.84])	07	
2.30	0.64		N^{14} 2.31 → 0	100	
			B^{11} 6.76 → 4.46[2.30]	17	
2.13	1.50		B^{11} 2.14 → 0	100	$1.24 \leq p < 1.40$
1.85			escape peak		
1.63			B^{12} 2.62 → 0.95[1.67][h]		
			B^{12} 1.67 → 0	100	
			N^{14} 3.95 → 2.31[1.64]	96	
1.4			K^{40}		
1.26			g		
0.97			B^{12} 0.95 → 0	100	
			B^{12} 2.62 → 1.67[0.95][h]		
0.83			C^{14} 6.89 → 6.09[0.80]	100	
			g		
0.74			N^{14} 5.83 → 5.10[0.73]	88	
			(C^{15} 0.66 → 0)		
			g		
0.62			C^{14} 7.35 → 6.72[0.62]		
			g		
0.51			annihilation radiation		

[a–g] Cf., Table I for explanation.
[h] R. R. Carlson and E. Norbeck (to be published).

is less than 5% of this peak.[11] The gamma decaying states in B^{10} are also populated very strongly. The comparison of the intensity analysis with particle data indicates that states in B^{11} are populated more than states in N^{14}.

There is a remarkable similarity in the relative population of C^{13} states from two dissimilar bombardments, $Be^9(Li^6,d)C^{13}$, $Q=9.2$ MeV and $B^{11}(Li^7,He^5)C^{13}$, $Q=9.0$ MeV. The ratio of the population of the 3.09-MeV state to the combined population of the 3.68- and 3.85-MeV states is 1.0:3.6 for Li^6+Be^9 and 1.0:4.8 for Li^7+B^{11}. These ratios are about equal within the estimated error of less than 50%. In both reactions, the 3.09 and 3.68–3.85 MeV peaks have the same appearance and have about the same intensity relative to the other gamma rays in the spectra. Particle data quoted by Morrison[12] gives the ratio of the population of the 3.09-MeV state to the combined population of the 3.68- and 3.85-MeV states formed in the former reaction as 1.0:3.3. A peak at 0.175 MeV from C^{13} 3.85 → 3.68 is listed in the table but not shown in the figures. This shows that the 3.85-MeV state in C^{13} is populated in this reaction.

[11] R. L. McGrath, Phys. Rev. **127**, 2139 (1962).
[12] G. C. Morrison, paper presented at the International Symposium on Direct Interactions and Nuclear Reaction Mechanisms, Padua, September 1962 (to be published).

Li^7+Be^9

The data are shown in Figs. 3 and 4 and summarized in Table II.

The gamma rays in the 3CPS spectrum can be accounted for by states in B^{11} and N^{14}. States in C^{13} and C^{14} are listed only as energetically possible sources of these gamma rays. There are gamma rays attributed to states in C^{14} and C^{13}, and B^{12} in the low-energy spectrum. The 4.46-MeV peak may have a sizeable contribution from the 4.43-MeV state in C^{12}, made in the reaction $Be^9(Li^7,H^4)C^{12}$. (The H^4 is presumably unbound.) The high-energy beta background from Li^8 and B^{12} is not entirely suppressed by the 3CPS and

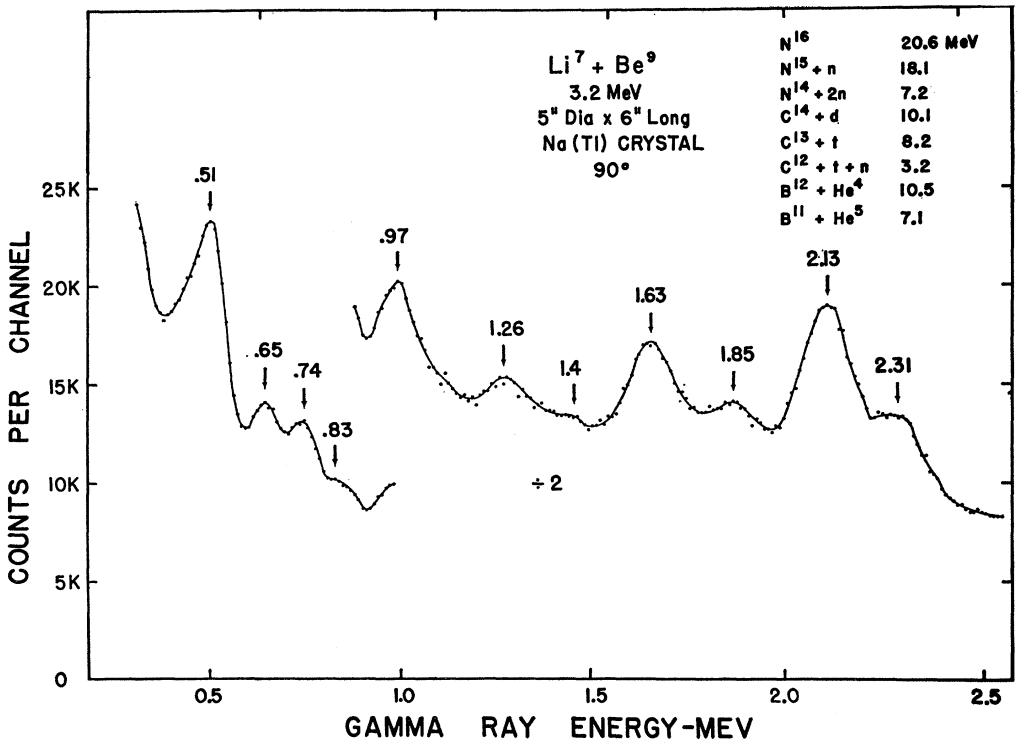

FIG. 3. Gamma rays with energies between 0.5 and 3 MeV from Li^7 bombardment of Be^9.

TABLE III. Li^6+B^{10}.

E_γ[a]	Relative intensity[b]	Component intensity[c]	Source[d]	Branching ratio[e]	Direct population[f]
9.1[h]	0.05		N^{15} 9.06 → 0	100	0.05
			9.16 → 0	100	
7.0	0.16		N^{14} 7.03 → 0	(100)	0.16
6.74	0.27		B^{11} 6.76 → 0	88	≤0.33
			C^{14} 6.72 → 0	100	
			(O^{15} 6.79 → 0)	100	
			(O^{15} 6.86 → 0)		
6.40	0.22		N^{14} 6.44 → 0	100	≤0.22
			(N^{14} 6.23 → 0)	24	
5.80	0.09	0.05	N^{14} 5.68 → 0	37	0.14
		0.04	N^{14} 5.83 → 0	15	0.26
5.10	1.00	≤0.41	N^{14} 5.10 → 0	67	≤0.61
			N^{14} 4.91 → 0	100	
			B^{11} 5.03 → 0		
4.46	1.85		B^{11} 4.46 → 0	100	
			C^{12} 4.43 → 0	100	
3.86	0.13		C^{13} 3.85 → 0	76	0.13
			3.68 → 0	100	
		0.01	N^{14} 3.95 → 0	04	
			N^{14} 6.23 → 2.31[3.92]	76	
3.36	0.09		N^{14} 5.68 → 2.31[3.37]	63	cf. 5.80γ
2.76	0.20		N^{14} 5.10 → 2.31[2.69]	33	cf. 5.10γ
			B^{11} 5.03 → 2.14[2.89]		
2.30	0.98		N^{14} 2.31 → 0	100	0[i]
		0.06	B^{11} 6.76 → 4.46[2.30]	17	
			(C^{11} 4.26 → 1.99[2.27])		
2.10	0.66		B^{11} 2.13 → 0	100	0.66
1.85			escape peak		
1.67	0.32		N^{14} 3.95 → 2.31[1.64]	96	0.33
1.47			K^{40}		
0.87			g		
0.74	0.22		N^{14} 5.83 → 5.10[0.73]	85	cf. 5.80γ
0.50			annihilation radiation		
0.18[h]			C^{13} 3.85 → 3.68[0.17]	24	cf. 3.86γ

[a–h] Cf., Table I for explanation.
[i] Assumed zero from isotopic spin considerations.

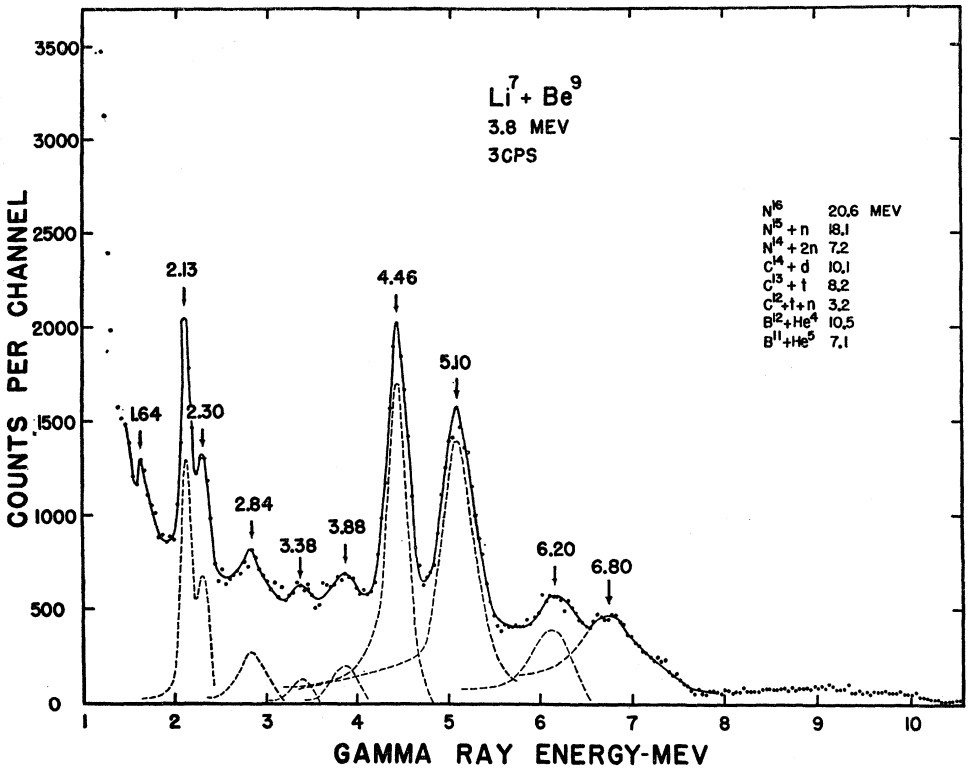

FIG. 4. Gamma rays with energies between 1 and 10 MeV from Li^7 bombardment of Be^9.

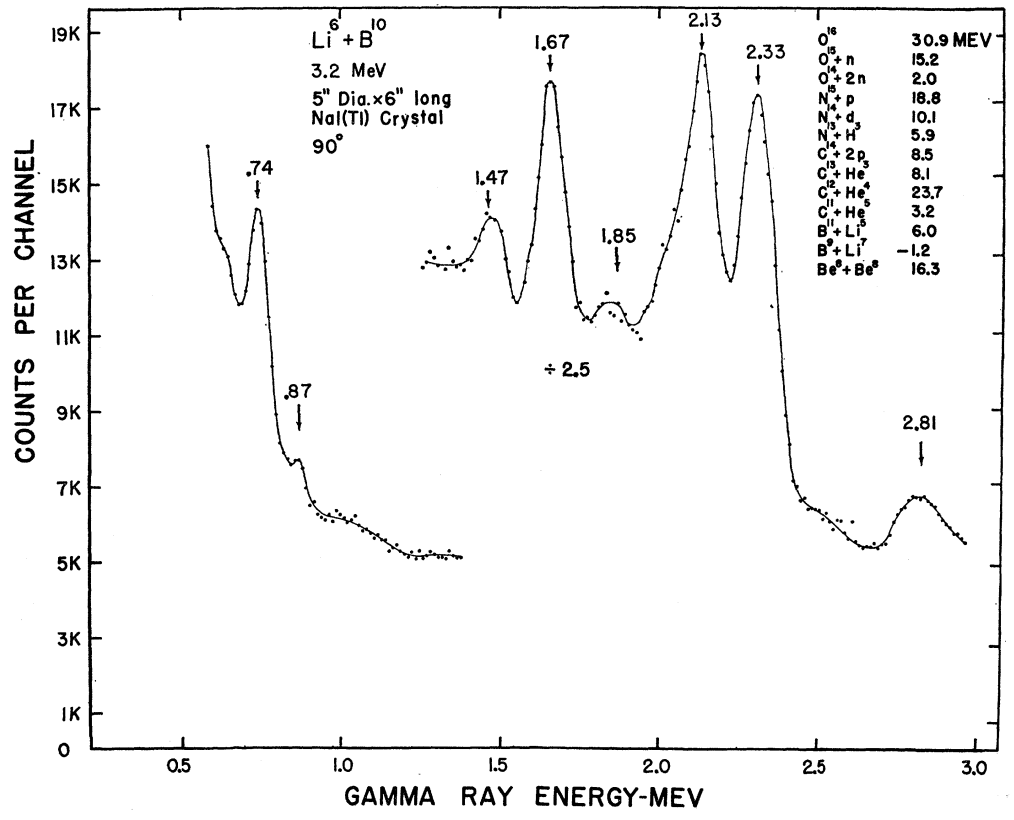

FIG. 5. Gamma rays with energies between 0.5 and 3 MeV from Li^6 bombardment of B^{10}.

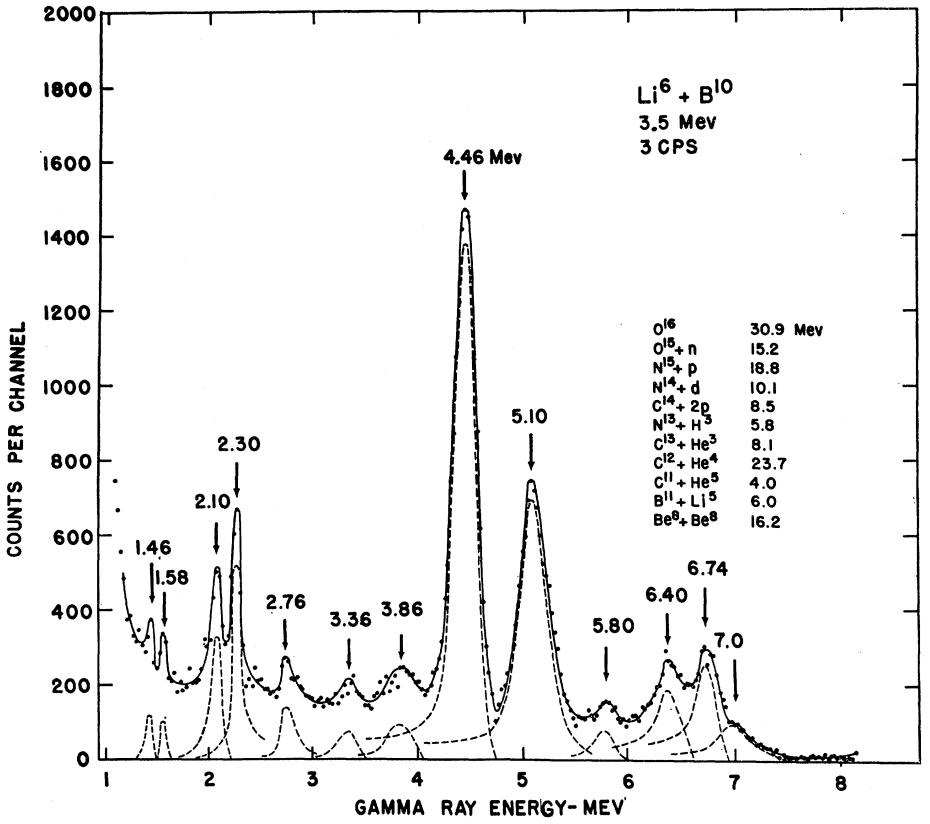

FIG. 6. Gamma rays with energies between 1 and 10 MeV from Li^6 bombardment of B^{10}.

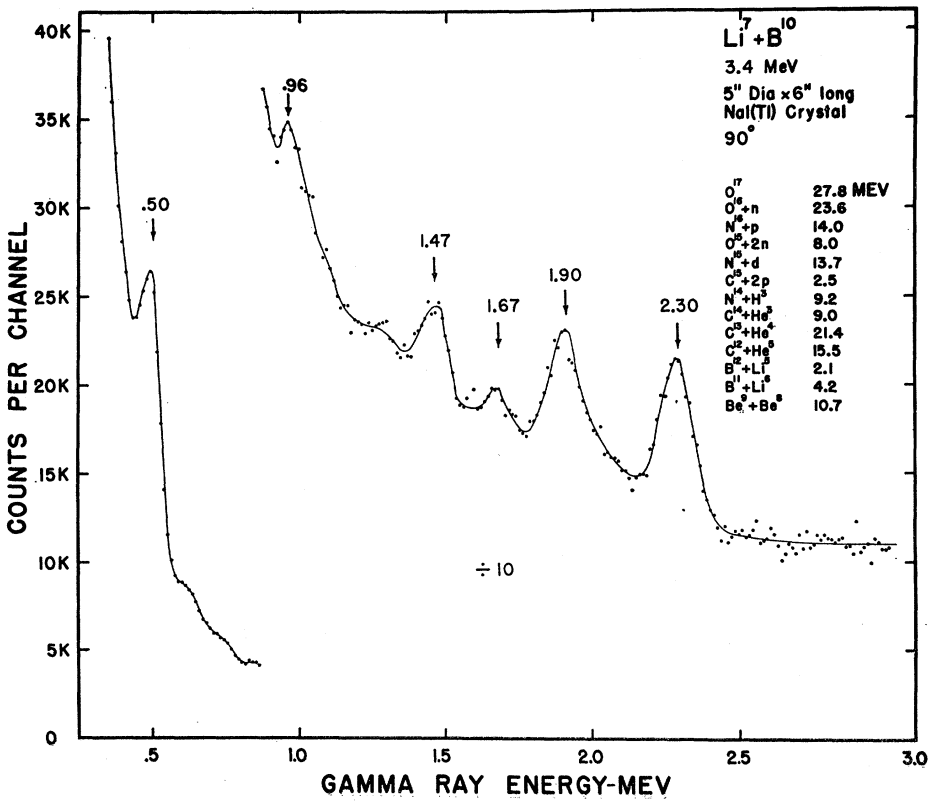

FIG. 7. Gamma rays with energies between 0.5 and 3 MeV from Li^7 bombardment of B^{10}.

TABLE IV. Li^7+B^{10}.

E_γ[a]	Relative intensity[b]	Component intensity[c]	Source[d]	Branching ratio[e]	Direct population[f]
9.76	0.20		N^{15} 9.83 → 0[h]	(100)	0.20
9.14	0.24		N^{15} 9.16 → 0		≤0.24
			9.06 → 0		
8.36	0.09		N^{15} 8.32 → 0	100	0.09
			8.57 → 0		
7.32	0.64		N^{15} 7.31 → 0	100	
7.03			N^{14} 7.03 → 0	(100)	
			O^{16} 7.12 → 0	100	
			6.92 → 0	100	
			(C^{14} 7.34 → 0)		
6.32	1.00		N^{15} 6.33 → 0	100	$0.9 \leq p \leq 1.00$
		≤0.04	N^{14} 6.23 → 0	24	
	unobservable	≤0.05	N^{14} 5.69 → 0	37	
5.28	2.89		N^{15} 5.30 → 0	100	≤2.37
			5.28 → 0	100	
			O^{15} 5.25 → 0, 5.20 → 0	100	
4.45	2.62		C^{12} 4.43 → 0	100	
			B^{11} 4.46 → 0	100	
3.80	0.18		C^{13} 3.85 → 0	76	
			(3.68 → 0)	100	
			O^{16} 10.94 → 7.12[3.82]	100	
			N^{14} 6.23 → 2.31[3.92]	76	
		≤0.01	N^{14} 3.95 → 0	04	
			N^{15} 9.16 → 5.28[3.88]		
3.38	0.10		N^{14} 5.69 → 2.31[3.38]	63	0.15
			N^{15} 8.57 → 5.28[3.29]		
2.25	0.68	≤0.42	N^{14} 2.31 → 0	100	assumed zero from isospin considerations
		≥0.26	N^{15} 7.57 → 5.28[2.29]	>90[i]	~0.3
1.82	0.36		N^{15} 7.16 → 5.28[1.88]	100	0.36
1.67	0.14		N^{14} 3.95 → 2.31[1.64]	96	≤0.14
			B^{12} 1.67 → 0	100	
1.47			K^{40}		
1.30			g		
1.04			g		
0.96			B^{12} 0.95 → 0	100	
0.85			g		
0.74			g		
			(B^{10} 0.72 → 0)	100	
0.63			g		
0.50			annihilation radiation		
			Li^7 0.48 → 0	100	

[a–g] Cf., Table I for explanation.
[h] See text Li^7+B^{10}.
[i] W. W. Eidson and R. D. Bent, Phys. Rev. **127**, 913 (1962).

appears as a long, low tail to the right of the gamma rays on the graph.

Li^6+B^{10}

The data are shown in Figs. 5 and 6 and summarized in Table III.

The spectrum from this reaction is due to levels in N^{14}, C^{13}, C^{12}, and B^{11}. The largest peak at 4.46 MeV is due to the 4.4-MeV levels in B^{11} and C^{12}. The proportion of B^{11} to C^{12} in this peak could not be determined from the data. Since the 2.31-MeV state in N^{14} is not expected to be formed because of isotopic spin considerations, the gamma radiation from this state was assumed to be part of cascades from higher states. This assumption was then used to obtain the population of some of these higher states. The observation of the 3.86-MeV gamma ray is evidence for the formation of C^{13} in the 3.85- and/or 3.68-MeV excited states. The 3.09-MeV state in C^{13} is not made with detectable intensity.

Li^7+B^{10}

The data are shown in Figs. 7 and 8 and summarized in Table IV.

All bound states in N^{15} seemed to be populated in this reaction. The two lowest gamma decaying states in B^{12} were populated. The largest peak is due to C^{12} and/or B^{11}. A triplet of 8.3-, 9.2-, and 9.8-MeV gamma rays appear in the Li^7+B^{10}, Li^6+B^{11}, and Li^7+C^{12} reactions along with gamma rays from levels in N^{15}. There are gamma decaying states in N^{15} at 9.06, 9.16, 8.57, and 8.31 and a bound state at 9.83 MeV whose de-excitation gamma rays have not been previously observed. The 9.8-MeV gamma rays are assigned to this state at 9.83 MeV in N^{15}.

It might be expected that the reaction $Li^7(B^{10},2n)O^{15}$

TABLE V. Li^6+B^{11}.

E_γ[a]	Relative intensity[b]	Component intensity[a]	Source[d]	Branching ratio[e]	Direct population[f]
9.40	0.59		N^{15} 9.83 → 0	100	
			O^{16} 9.58 → 0	100	
8.90	1.22		N^{15} 9.06 → 0		
			9.16 → 0		
7.30	0.28		N^{15} 7.31 → 0	100	0.28
7.0?	0.26		O^{16} 7.12 → 0	100	
			6.92 → 0	100	
6.34	1.00		N^{15} 6.33 → 0	100	$0.88 \leq p \leq 1.00$
		0.07	N^{14} 6.23 → 0	24	
			(O^{15} 6.15 → 0)	100	
	unobservable	≤0.05	N^{14} 5.69 → 0	37	
5.26	4.71		N^{15} 5.31 → 0	100	≤4.07
			5.28 → 0	100	
			O^{15} 5.25 → 0	100	
			5.20 → 0	100	
4.48	6.35		C^{12} 4.43 → 0	100	6.35
3.90	0.23		C^{13} 3.85 → 0	76	
			3.68 → 0	100	
			N^{14} 6.23 → 2.31[3.92]	76	
			O^{16} 10.94 → 7.12[3.82]	100	
			N^{15} 9.16 → 5.28[3.88]		
		0.004	N^{14} 3.95 → 0	4	
3.40	0.09		N^{14} 5.69 → 2.31[3.37]	63	≤0.14
			N^{15} 8.57 → 8.28[3.29]		
2.31	0.40		N^{14} 2.31 → 0	100	
			N^{15} 7.57 → 5.28[2.29]	>90[h]	
1.89	0.25		N^{15} 7.16 → 5.28[1.88]	100[i]	≤0.25
			escape peak		
1.64	0.10		N^{14} 3.95 → 2.31[1.64]	96	0.10
1.46			K^{40}		
1.26			g		
1.01			g		
0.83			g		
0.73			g		
			N^{14} 5.83 → 5.10[0.73]	85	
0.63			g		
0.51			annihilation radiation		

[a–g] Cf., Table I for explanation.
[h] W. W. Eidson and R. D. Bent, Phys. Rev. 127, 913 (1962).
[i] D. F. Hebbard, Nucl. Phys. 19, 511 (1960).

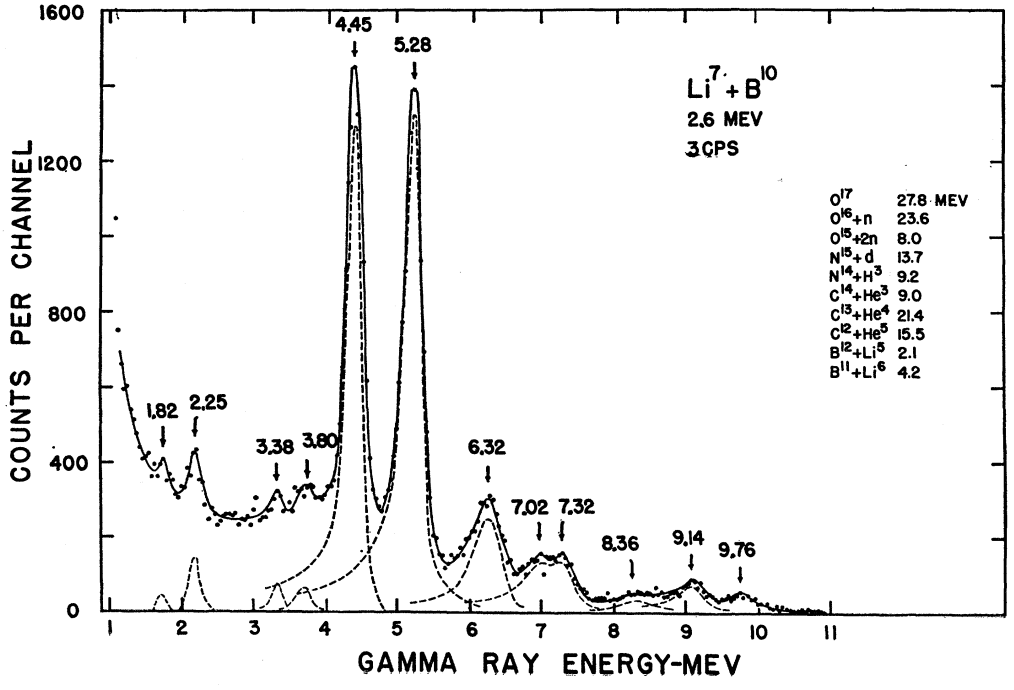

FIG. 8. Gamma rays with energies between 1 and 10 MeV from Li^7 bombardment of B^{10}.

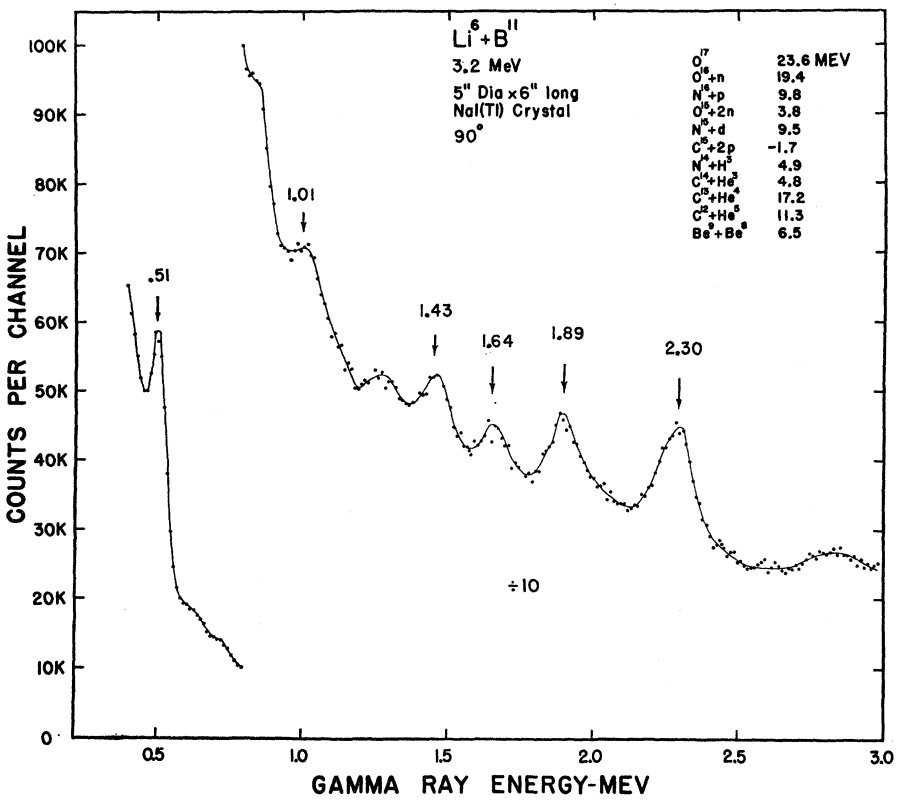

FIG. 9. Gamma rays with energies between 0.5 and 3 MeV from Li^6 bombardment of B^{11}.

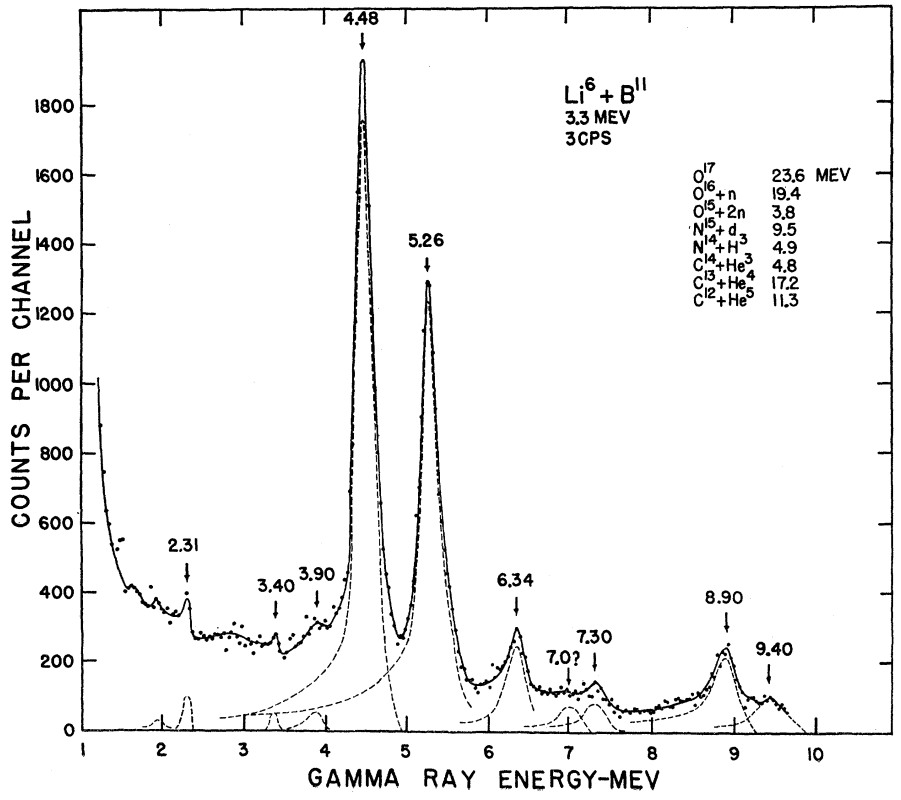

FIG. 10. Gamma rays with energies between 1 and 10 MeV from Li^6 bombardment of B^{11}.

TABLE VI. Li^7+B^{11}.

E_γ[a]	Relative intensity[b]	Component intensity[c]	Source[d]	Branching ratio[e]	Direct population[f]
8.88	0.45		N^{15} 9.06 → 0	100	
			9.16 → 0	100	
		≤0.02	O^{16} 8.88 → 0	07	≤0.30
6.98	1.00		O^{16} 6.92 → 0	100	0.94≤p≤1.00
			7.12 → 0	100	
6.13	1.42		O^{16} 6.14 → 0	100	≤1.14
			C^{14} 6.09 → 0	100	
		<0.06	Be^{10} 5.96 → 0	22	
			(N^{15} 6.33 → 0)	100	
5.25	0.34		N^{15} 5.30 → 0	100	0.34
			5.28 → 0	100	
4.46	0.40		C^{12} 4.43 → 0	100	0.40
3.85	3.10		C^{13} 3.85 → 0	76	3.10
3.67			3.68 → 0	100	
			(O^{16} 10.95 → 7.12)[3.83]	100	
			(O^{17} 3.85 → 0)	100	
3.34	0.33		Be^{10} 3.37 → 0	100	0.22≤p≤0.33
3.05	0.64		C^{13} 3.09 → 0	100	0.64
2.67	0.22		O^{16} 8.88 → 6.14[2.74]	74	<0.30
			Be^{10} 5.96 → 3.37[2.59]	78	<0.28
2.2			O^{17} 3.06 → 0.87[2.18]	100	
			N^{15} 7.57 → 5.28[2.29]	>90[h]	
			(B^{11} 2.14 → 0)	100	
1.87			O^{16} 8.88 → 7.12[1.76]	14	
			8.88 → 6.92[1.96]	5	
			(N^{15} 7.16 → 5.28[1.78])	100[i]	
1.1–1.3			[g]		
1.0			[g]		
0.81			[g]		
			(O^{17} 0.87 → 0)	100	
0.72			[g]		
0.60			[g]		
0.50			annihilation radiation		
			Li^7 0.48 → 0	100	

[a–g] Cf., Table I for explanation.
[h] W. W. Eidson and R. D. Bent Phys. Rev. **127**, 913 (1962).
[i] D. F. Hebbard, Nucl. Phys. **19**, 511 (1960).

would be as prolific as $Li^7(B^{10},d)N^{15}$, but this is not the case. While the gamma rays from N^{15} are a prominent part of the spectrum, the expected gamma rays from O^{15} at 6.16, 6.79, and 7.55 MeV are not seen at all.

Li^6+B^{11}

The data are shown in Figs. 9 and 10 and summarized in Table V.

The two largest peaks are mostly from the first excited states in C^{12} and N^{15}. These same two peaks are the prominent ones in the conjugate reaction Li^7+B^{10}. There is a remarkable similarity in the spectra from these two reactions. This similarity leads us to suggest the presence of gamma rays of about 7.0 MeV in the Li^6+B^{11} spectrum due to O^{16}, 6.92 → 0 and 7.12 → 0. The intensity of this gamma-ray may be estimated from the height of the plateau just to the left of the 7.30-MeV gamma-ray peak. Similarly, the 8.90- and 9.40-MeV peaks have been assigned to the 9.06-, 9.16-, and 9.83-MeV states in N^{15}. The 8.88-MeV level in O^{16} cannot contribute to this peak since its cascade by way of the 6.13-MeV level is not seen with any appreciable intensity. The calibration for this particular spectrum is somewhat uncertain in the 8–9 MeV range.

The very large peak at 5.26 MeV may contain contributions from the doublet in O^{15}. The higher levels in O^{15} are energetically forbidden.

Li^7+B^{11}

The data are shown in Figs. 11 and 12 and the intensity analysis is given in Table VI.

The largest peaks in the spectrum are due to gamma rays from levels in C^{13} and O^{16}. The 8.88-MeV peak cannot have a sizeable contribution from the 7% decay of the 8.88-MeV level in O^{16} to the ground state and must be assigned to N^{15} 9.06 → 0 and 9.16 → 0. The relative population of gamma decaying states in the residual nuclei formed are as follows: C^{13}—~3.74, O^{16}—~2.74, N^{15}—0.77, C^{12}—0.40, and Be^{10}—0.39. The Be^{10} formed requires the transfer of mass from B^{11} to Li^6 if the reaction is a direct interaction.

Li^6+C^{12}

The data are shown in Figs. 13 and 14, and the intensity analysis is given in Table VII.

All gamma rays have been assigned to states in N^{14} and O^{17}.

The gamma-decay mode of the 7.40-MeV state in N^{14} has not been definitely established. A cascade from the

TABLE VII. Li^6+C^{12}.

E_γ[a]	Relative intensity[b]	Component intensity[c]	Source[d]	Branching ratio[e]	Direct population[f]
7.40	0.07		N^{14} 7.40 → 0	(100) I	0.07 I[h]
				80 II	0.36 II
6.97	0.52		N^{14} 7.03 → 0	(100)	≤0.52
			(O^{16} 6.92 → 0)	100	
			(O^{16} 7.12 → 0	100	
6.52	1.00		N^{14} 6.44 → 0	78 I	1.29 I
				100 II	1.00 II
6.1	0.10		N^{14} 6.23 → 0	24	≤0.42
			(O^{16} 6.14 → 0)	100	
5.82 }	~0.2	0.05	N^{14} 5.83 → 0	15	0.36
5.70 }		0.15	N^{14} 5.69 → 0	37	cf. 3.40γ
5.14	0.83	0.42	N^{14} 5.10 → 0	67	cf. 2.78γ
			N^{14} 4.91 → 0	100	0.41 I
					0.13 II
3.94	0.59	≤0.32	N^{14} 6.23 → 2.31[3.92]	76	cf. 6.1
			O^{17} 3.85 → 0		
		0.03	N^{14} 3.95 → 0		
3.40	0.26		N^{14} 5.69 → 2.31[3.38]	63	0.41
2.78	0.20		N^{14} 5.10 → 2.31[2.69]	33	0.62
2.50	0.29		I N^{14} 6.44 → 3.95[2.49]	22	cf. 6.52γ
			II N^{14} 7.40 → 4.90[2.50]	80	cf. 7.40γ
2.31	2.06		N^{14} 2.31 → 0	100	
			O^{17} 3.07 → 0.87[2.20]	100	
1.80			escape peak		
1.64	0.66		N^{14} 3.95 → 2.31[1.64]	96	0.10 I
					0.39 II
1.43			K^{40}		
1.35			g		
0.87	0.25		O^{17} 0.87 → 0	100	
0.72	0.31		N^{14} 5.83 → 5.10[0.73]	85	cf. 5.14γ
0.51			annihilation radiation		

[a–g] Same as Table I.
[h] I and II refer to the proposed sources of the 2.50γ. See text.

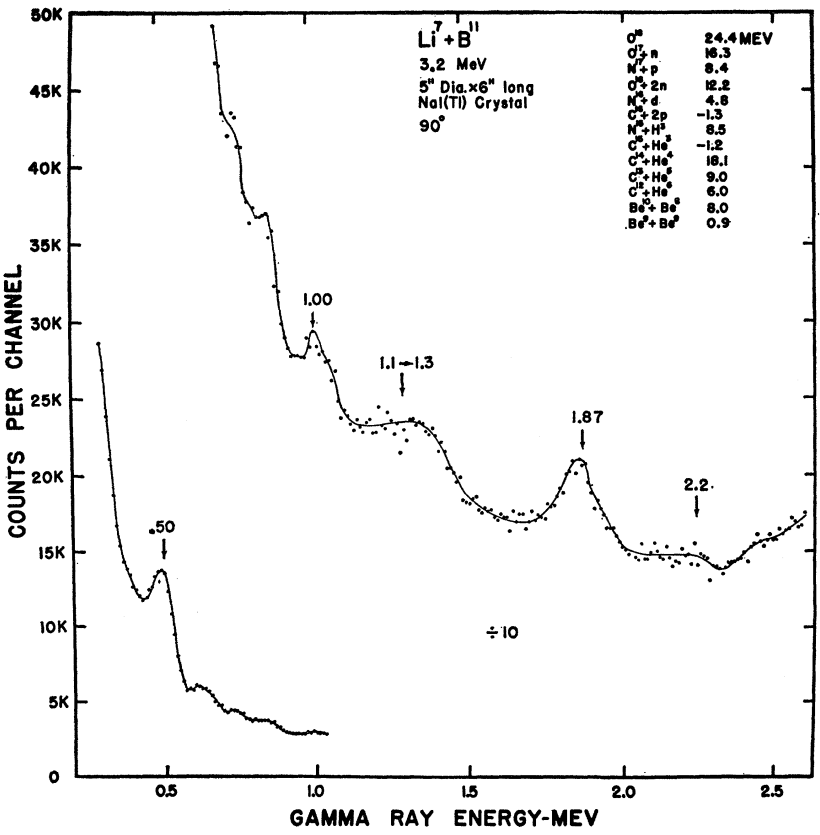

FIG. 11. Gamma rays with energies between 0.5 and 3 MeV from Li^7 bombardment of B^{11}.

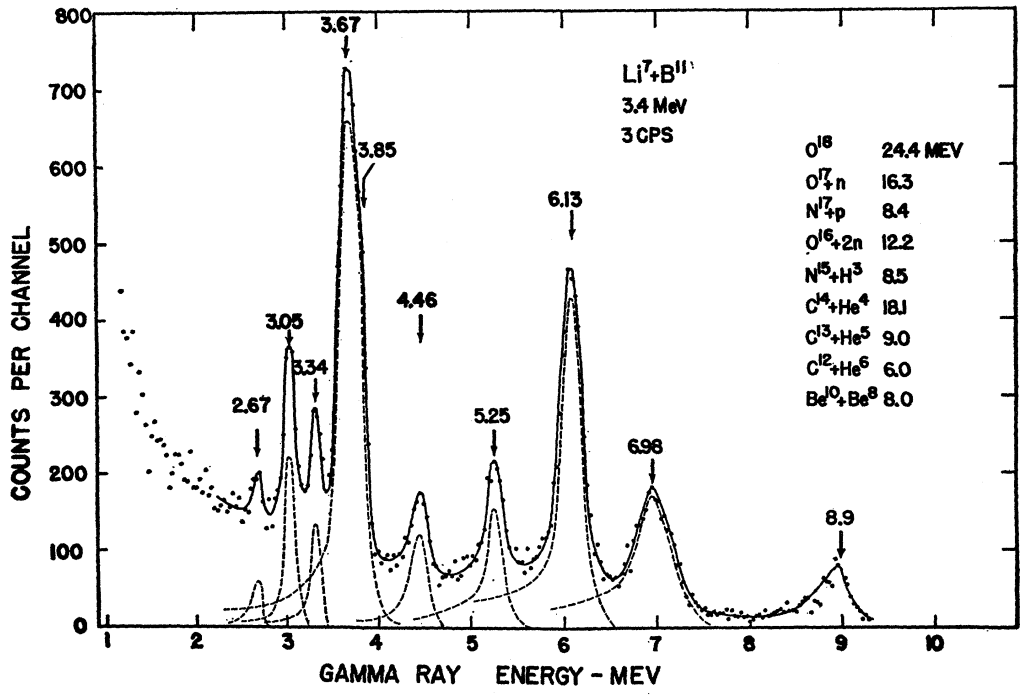

FIG. 12. Gamma rays with energies between 1 and 10 MeV from Li^7 bombardment of B^{11}.

7.40-MeV state to the 4.90-MeV state would account for the 2.52-MeV gamma ray which appears on both the 3CPS spectrum and the low-energy spectrum. The branching ratio indicated by the intensity analysis is 7.40 → 4.90, 80%; 7.40 → 0, 20%. There are three other possible cascades from the 7.40-MeV state which have energies corresponding to observed gamma rays, 7.40 → 5.10, 7.40 → 3.95, and 7.40 → 2.31. However, these gamma rays can be better accounted for by other sources. Another possible source for the 2.52-MeV

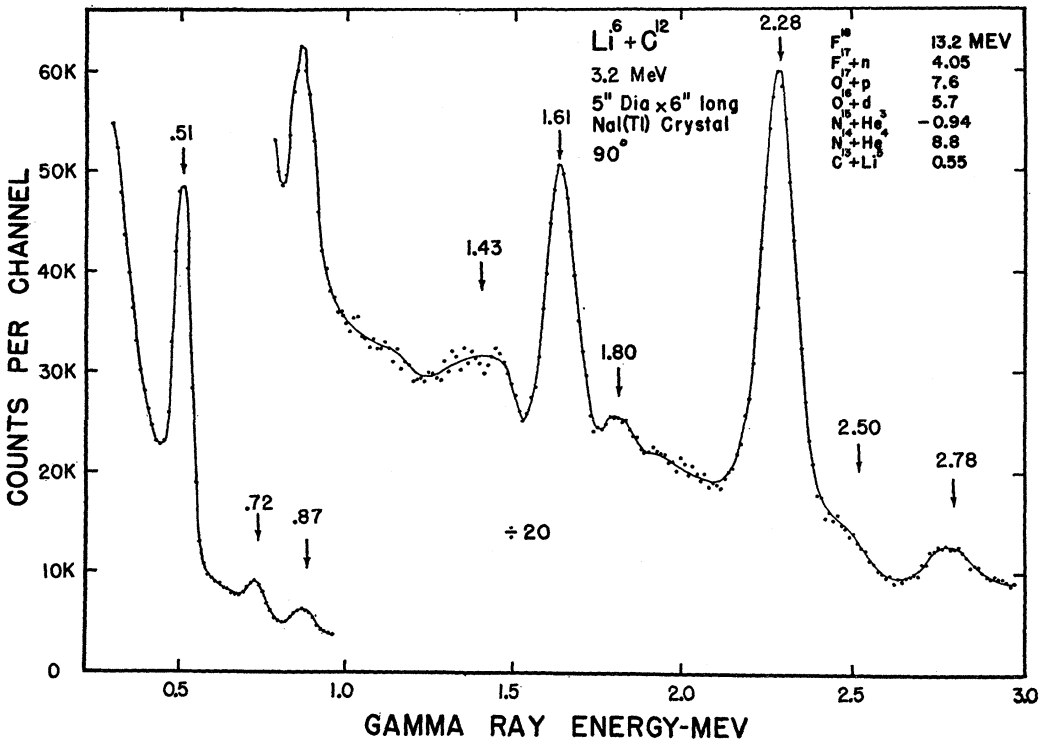

FIG. 13. Gamma rays with energies between 0.5 and 3 MeV from Li^6 bombardment of C^{12}.

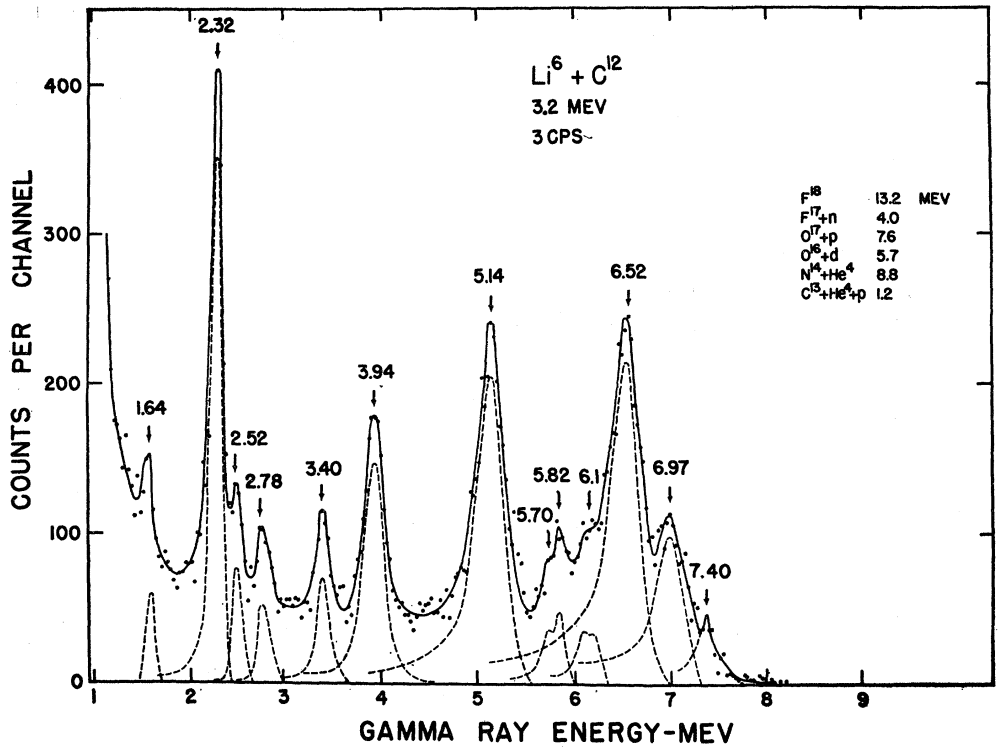

FIG. 14. Gamma rays with energies between 1 and 10 MeV from Li^6 bombardment of C^{12}.

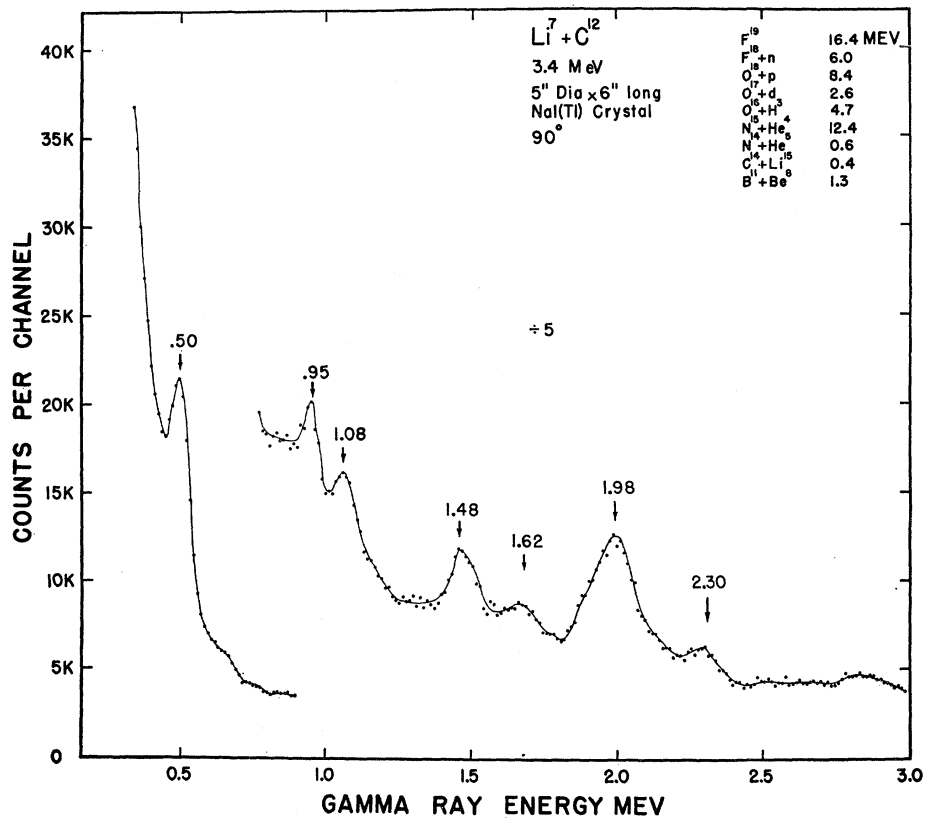

FIG. 15. Gamma rays with energies between 0.5 and 3 MeV from Li^7 bombardment of C^{12}.

TABLE VIII. Li^7+C^{12}.

E_γ[a]	Relative intensity[b]	Component intensity[c]	Source[d]	Branching ratio[e]	Direct population[f]
9.86	1.66		N^{15} 9.83 → 0	(100)	1.66
9.16	1.43		N^{15} 9.16 → 0		
			9.06 → 0	100	0.25
8.54	0.25		N^{15} 8.57 → 0	}	
			(8.31 → 0)	100 }	
7.31	0.45		N^{15} 7.31 → 0	100	0.45
6.32	1.00		N^{15} 6.33 → 0	100	
5.28	5.30		N^{15} 5.30 → 0	100	1.44[h]
			5.28 → 0		
4.52	1.02		N^{15} 10.82 → 6.33[4.49]		
			O^{18} 4.45 → 0	(100)	
3.88	0.50		F^{18} 3.85 → 0	(100)	
			N^{15} 9.16 → 5.28[3.88]		
3.32	1.32		F^{18} 3.35 → 0	(100)	
			N^{15} 8.57 → 5.28[3.24]		
2.24	1.32		N^{15} 7.57 → 5.28[2.29]	>90[i]	≤1.45
			O^{17} 3.06 → 0.87[2.19]	100	
			F^{18} 2.10 → 0	30	
			(B^{11} 2.15 → 0)	100	
			(N^{14} 2.31 → 0)	100	
1.94	4.4		N^{15} 7.16 → 5.28[1.88]	100[j]	<4.4
			O^{18} 1.98 → 0	100	
			N^{15} 9.16 → 7.57[1.59]		
1.67	0.98		F^{18} 1.70 → 0	30	
			O^{18} 3.55 → 1.98[1.57]	100	
1.48			K^{40}		
1.08	0.65		F^{18} 1.08 → 0	100	
			1.04 → 0	100	
			F^{18} 2.10 → 1.08[1.02]	35	
			2.10 → 1.04[1.06]	35	
			[g]		
			N^{15} 6.33 → 5.31[1.02]		
0.95	0.98		F^{18} 0.94 → 0	100	
0.87	0.28		O^{17} 0.87 → 0	100	
			[g]		
0.65			N^{15} 9.83 → 9.17[0.66]		
			F^{18} 1.70 → 1.04[0.66]	70	
0.50			annihilation radiation		
			Li^7 0.48 → 0	100	

[a–g] Cf., Table I for explanation.
[h] R. K. Hobbie and F. W. Forbes, Phys. Rev. **126**, 2137 (1962).
[i] W. W. Eidson and R. D. Bent, Phys. Rev. **127**, 913 (1962).
[j] D. F. Hebbard, Nucl. Phys. **19**, 511 (1960).

gamma ray is a cascade from the 6.44-MeV state to the 3.95-MeV state in N^{14}.

Li^7+C^{12}

The data are shown in Figs. 15 and 16 and summarized in Table VIII.

Comparison of this spectrum with that of Li^7+B^{10} and Li^6+B^{11} shows that gamma rays from the levels in N^{15} above the 5.3-MeV doublet are stronger relative to the doublet in the Li^7+C^{12}. Particle data indicates that the 5.3-MeV doublet is populated 1.44 times as much as the 6.33-MeV level.[9] Therefore, the very large 5.28-MeV peak is largely from cascades to the 5.3-MeV doublet from the 7.16- and 7.57-MeV levels. The 1.94-MeV gamma peak is much larger in this spectrum than either of these two comparison spectra. This may be from a greater population of the 7.57-MeV level in N^{15} or the formation of the 1.98-MeV level in O^{18}.

Eidson[13] notes that the 8.31-MeV state in N^{15} is thought to be the mirror level of the 7.55-MeV state in O^{15} which has an $E1$ matrix element of 4×10^{-6} Weisskopf units which is the smallest known. The spectra from N^{15} formed in the reactions $C^{12}(Li^7,\alpha)N^{15}$, $B^{10}(Li^7,d)N^{15}$, and $B^{11}(Li^6,d)N^{15}$ show little or no evidence for the ground-state transition of the 8.31-MeV state. This implies either that the state is not formed at all or that it has an anomalously weak ground-state transition as would be expected from the properties of its mirror.

Gamma rays from F^{18} and O^{17} may be seen. The 3.32-MeV peak can be assigned to the gamma decay of the 3.35-MeV state in F^{18}. This bound state has not been observed to gamma decay before. It may be due to a transition in N^{15}, however. The 4.52-MeV gamma ray may be due to a cascade from the 10.82-MeV level in N^{15} and/or the previously unobserved gamma decay at the 4.45-MeV level in O^{18}.

[13] W. W. Eidson (private communication).

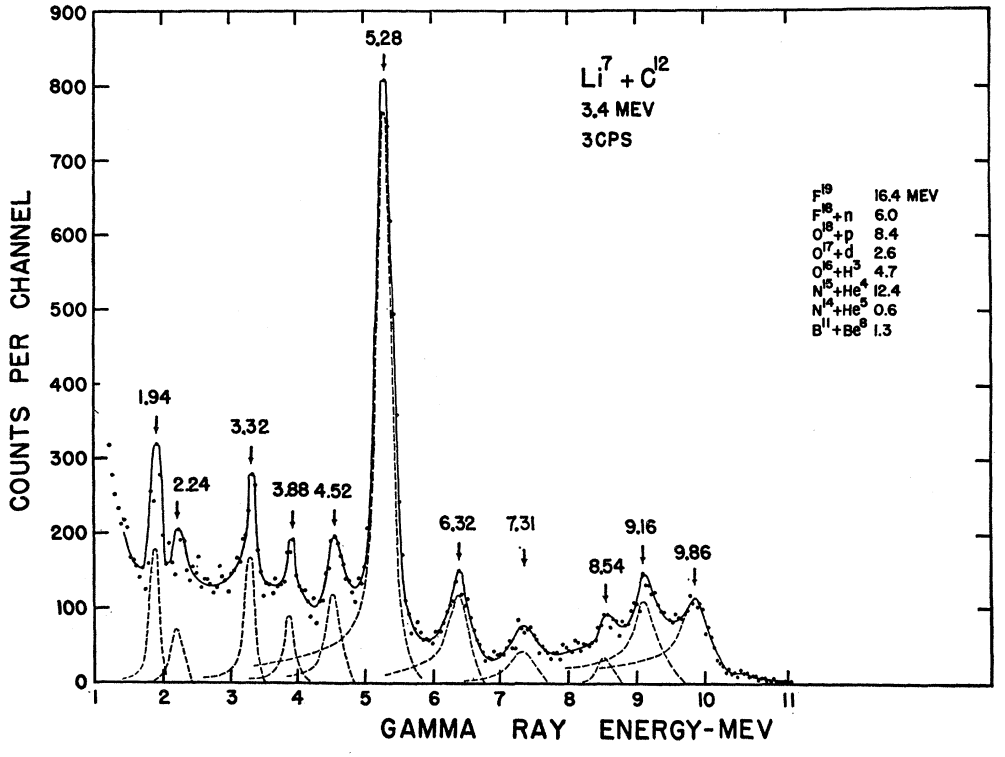

FIG. 16. Gamma rays with energies between 1 and 10 MeV from Li^7 bombardment of C^{12}.

CONCLUSIONS

Although other investigators have found some evidence of compound nucleus effects,[14] most of the reactions seem to proceed by the transfer of a small number of nucleons from one nucleus to the other. The observations presented here follow the general rule noted previously[1,15] that for any given beam-target pair, the reaction yield depends on the amount of matter transferred. A detailed analysis indicates, however, that other factors must also be important. For example, with the reactions $B^{10}(Li^7,d)N^{15}$ and $B^{10}(Li^7,2n)O^{15}$ leading to mirror states in N^{15} and O^{15}, the reaction giving off the deuteron is considerably more prolific than the reaction giving off two neutrons. The two dissimilar reactions $Be^9(Li^6,d)C^{13}$ and B^{11}-$(Li^7,He^5)C^{13}$ produce the 3.09-MeV and the 3.68- and/or 3.85-MeV levels in C^{13} with about the same relative populations. This may reflect properties of these levels in this residual nucleus rather than the reaction mechanism. Generally, transfer of mass can occur from either nucleus to the other but the reactions Be^9-$(Li^6,Be^8)Li^7$ and $B^{11}(Li^7,Be^8)Be^{10}$ require a transfer of mass from the target nucleus to the bombarding particle.

Table IX summarizes the observations on gamma-ray emission observed for lithium bombardment of these light elements. The sources of gamma radiation listed in Table IX can account for at least 90% of the observed radiation in all cases and usually can account for all. This listing of sources is not meant to imply that other energetically possible sources have been ruled out. It means that it is possible to account for the observed radiation on the basis of these relatively few reactions.

TABLE IX. Significant sources of observed gamma raidation.

Beam and target	Residual nuclei giving gamma radiation				
Li^6+Be^9	$Li^{7*}+Be^8$,	$B^{10*}+He^5$,	$B^{11*}+\alpha$,	$C^{13*}+d$	
Li^7+Be^9		$B^{11*}+He^5$,	$B^{12*}+\alpha$,	$N^{14*}+2n$	
Li^6+B^{10}		$B^{11*}+Li^5$,	$C^{12*}+\alpha$,	$N^{14*}+d$	
Li^7+B^{10}		$C^{12*}+He^5$,	$C^{13*}+\alpha$,	$N^{15*}+d$	
Li^6+B^{11}		$C^{12*}+He^5$,	$C^{13}+\alpha$,	$N^{15*}+d$	
Li^7+B^{11}	$Be^{10*}+Be^8$,	$C^{12*}+He^5$,	$C^{13*}+He^5$,	$N^{15*}+t$,	$O^{16*}+d$
Li^6+C^{12}		$N^{14*}+\alpha$,	$O^{17*}+p$		
Li^7+C^{12}		$N^{15*}+\alpha$,			

[14] J. M. Blair and Russel K. Hobbie, Phys. Rev. **128**, 2282 (1962).

[15] E. Norbeck, Phys. Rev. **121**, 824 (1961).